International Journal of Control, Automation, and Systems (2011) 9(4):701-708 http://www.springer.com/12555
DOI 10.1007/s12555-011-0411-0

A Closed-form Method for the Attitude Determination Using GNSS Doppler Measurements

Byungwoon Park, Sanghoon Jeon, and Changdon Kee*

Abstract: The fixing process for cycle ambiguity is a major issue for attitude determination using multiple Global Navigation Satellite System (GNSS) antennas. Existing algorithms have used pseudorange with large noise and ambiguity-included carrier phase measurements so the volume of the ambiguity search space is inevitably large. We propose a new algorithm to determine the attitude of a rotating vehicle using Doppler measurement in a closed form. Using differential and angular velocity estimation, we can reduce the size of the search space and the number of ambiguity candidates. We present simulation results using one master and two slave GNSS antennas. For all the cases in our simulations, the probability of one epoch fix is over 97%. Moreover, we achieved resolution of the ambiguity in two consecutive epochs. In other words, the maximum time-to-first-fixed-attitude (TTFFA) of our algorithm is only two seconds. Our algorithm can reduce the computation load in the ambiguity resolution for rotational vehicle attitude; consequently, it will be helpful in rapid and accurate determination in a case of phase lock loss due to a complex maneuver such as a fast spin.

Keywords: Ambiguity resolution, attitude determination, Doppler, GPS, rotating vehicle.

1. INTRODUCTION

Precise attitude determination is required in connection with numerous marine, airborne, and all kinds of agricultural and industrial equipment applications. Such vehicle attitude information has often been obtained by inertial measurement units (IMUs). These systems are very precise, but the high cost and calibration load are major obstacles to widespread usage.

GNSS is a cheap and precise sensor and this has been suggested as an alternative to IMU. Accurate attitude determination has emerged as an important application of GNSS. Researchers have examined attitude determination methods for single and multiple antennas. The single GNSS antenna method is derived from velocity and acceleration based on GPS position, velocity, and time. A vehicle can estimate its own attitude without resolution of ambiguity in the carrier phase, but it suffers overshoot and time delay by filtering and includes bias in its angles of attack and sideslip.

The multiple antenna method overcomes the limitation of single antenna-based attitude determination. Paired antennas are placed on a rigid body, and the baseline vectors between each pair are known quantities within the body-frame coordinates. If carrier phase measurements are taken from each antenna the integer ambiguities may be resolved to determine the baseline vectors. Ambiguity of attitude is easily resolved relative to that of the position, because the baseline of the antennas is a known short distance [8]. It is possible to estimate attitude to within an accuracy of 0.5 degree after such an ambiguity resolution.

Dedicated GPS attitude receivers have been developed since the 1990s. During the last 10 years, they have shown significant capability as independent sensors for attitude determination for RADCAL (RADar CALibration), GADACS (GPS Attitude Determination And Control System), and REX-II (Radiation Experiment II) satellites amongst other applications. It has been recently shown that non-dedicated GPS boards or such assemblies with low-cost chipsets have a good performance as attitude sensors [1]. It remains difficult to quickly search cycle ambiguity within a given hardware capacity, and effective reduction of the computational load remains an issue.

Generally, pseudorange and carrier phase observables have been used to determine the attitude. However, Doppler rather than these measurements would be greatly helpful in reducing the computation load since Doppler observables involve neither large amounts of noise as pseudorange nor ambiguity of integrated carrier phase. Integrated carrier phase is measured by counting the number of whole wavelengths after initial signal lock-on and through addition of the instantaneous change in re-

Manuscript received June 3, 2010; revised February 22, 2011; accepted April 25, 2011. Recommended by Editorial Board member Young Jae Lee under the direction of Editor Jae-Bok Song. This work was supported by Korea Aerospace Research Institute through KARI's University Partnership Program contracted through the Institute of Advanced Aerospace Technology at Seoul National University.

Byungwoon Park is with the Cadastral Research Inst., Korea Cadastral Survey Corp., #812-5 Manhattan (Yeoeuido Dept.) Bldg. 33, Yeoeui 1gil, Yeongdeungpo-gu, Seoul, Korea (e-mail: byungwoon.park@gmail.com).
Sanghoon Jeon and Changdon Kee are with the School of Mechanical and Aerospace Engineering and SNU-IAMD, Seoul National University, Bldg. 301-1410 Gwanak 599 Gwanak-ro, Gwanak-gu, Seoul 151-742, Korea (e-mails: {dori8011, kee}@snu.ac.kr).
* Corresponding author.

ceiver-to-satellite distance which is seen in the Doppler signal. It is a biased range because the initial number of whole integer wavelengths is unknown, in the same manner as a remaining constant of integration. The method of removing the integration constant is by differentiating the integrated function. In the same way, Doppler measurement, which can be obtained by the differentiating the carrier phase, can help find ambiguity-free solutions in GPS applications. Velocity determination based upon Doppler effects or Doppler shift derived from the carrier phase shows very precise results.

Doppler shift measurement occurs in a velocity domain, whereas position or attitude determination using multiple antennas requires to be estimated in a distance domain. The distance change into velocity is derived through only a rotation, and we apply this idea to the attitude determination of a rotating vehicle. This paper first introduces a method to determine the attitude using Doppler shift measurement, and then explains how to apply this algorithm. Thereafter our simulation shows the reality of its feasibility.

We suggest a closed-form method for attitude determination using GNSS Doppler effect measurements, which is greatly different to existing approaches. Our emphasis in this paper is the feasibility of removing the ambiguity-searching process. In a real system, we cannot avoid measurement and estimation error so we apply the algorithm to reduce the number of candidates. It would be helpful to resolve the cycle ambiguity in one epoch.

2. ATTITUDE DETERMINATION METHOD USING DOPPLER MEASUREMENTS

2.1. Velocity determination using doppler measurements

The relative motion of a satellite and an observer causes change in the observed frequency of the satellite signal. This Doppler shift is measured routinely in the carrier tracking loop of a GPS receiver [2].

$$\dot{\phi}^{(k)} = \dot{d}^{(k)} + (\dot{B} - \dot{b}^{(k)}) + \dot{I}^{(k)} + \dot{T}^{(k)} + n_{\dot{\phi}^{(k)}}, \qquad (1)$$

$\dot{d}^{(k)}$: geometric range rate between the receiver and the k-th satellite,

$\dot{B}$: receiver clock drift,

$\dot{b}^{(k)}$: the k-th satellite clock drift,

$\dot{I}^{(k)}$: ionospheric delay rate for the k-th satellite,

$\dot{T}^{(k)}$: tropospheric delay rate for the k-th satellite,

$n_{\dot{\phi}^{(k)}}$: receiver system noise for the k-th satellite.

Given the satellite velocity, the Doppler shift can be used to estimate the user velocity. The Doppler measurement or, equivalently, the range rate ($\dot{\phi}(k)$), can be written as a projection of the relative velocity vector on the satellite line-of-sight vector:

$$\dot{\phi}(k) = (v^{(k)} - v) \cdot e^{(k)} + \dot{B} + \delta\dot{\phi}^{(k)}, \qquad (2)$$

$v^{(k)}$: satellite velocity vector, known from the navigation message broadcast by the satellite [3]

v: user velocity, to be estimated

$e^{(k)}$: user to satellite line-of-sight unit vector

$\delta\dot{\phi}^{(k)}$: combined error due to the satellite clock, ionosphere, troposphere, and measurement noise.

Equation (2) is linear in observer velocity components and can be expressed as:

$$\dot{\phi}(k) - v^{(k)} \cdot e^{(k)} = -v \cdot e^{(k)} + \dot{B} + \delta\dot{\phi}^{(k)}. \qquad (3)$$

Denoting $(\dot{\phi}^{(k)} - v^{(k)} \cdot e^{k})$ as $z^{(k)}$, (3) can be compactly written as a set of equations in a matrix notion as:

$$z^{(k)} = [-e^{(k)} \;\; 1]\begin{pmatrix} v \\ \dot{B} \end{pmatrix} + \delta\dot{\phi}^{(k)} = H\begin{pmatrix} v \\ \dot{B} \end{pmatrix} + \delta\dot{\phi}^{(k)}. \qquad (4)$$

The matrix H is the observation matrix, and 1 is a column vector having 1s as its elements. The observer velocity can be estimated by the least-square solution, and this inevitably suffers from the combined error, $\delta\dot{\phi}^{(k)}$. To reduce this error various methods are helpful such as estimation of the precise velocity of a GPS satellite or an atmospheric prediction model [4]. Generally, the Doppler derived from the carrier phase is used for velocity estimation instead of the receiver-generated measurement because the latter is usually noisier than the former.

In this paper, we do not need to use methods other than that of (4) because the differential velocity observed between multiantennas can reduce the common error. The Doppler derived from the carrier phase was determined by fitting a curve using second order polynomials with successive phase measurements.

2.2. Attitude determination for the rotation-only vehicle

The attitude angles describe the orientation of the vehicle frame with respect to the local level navigation frame. Once two baseline vectors are estimated accurately, the attitude of the vehicle is easily determined. To explain our attitude determination algorithm using Doppler shift measurement, we introduce a rotation-only vehicle as shown in Fig. 1. Two GPS antennas are rotated about a fixed axis.

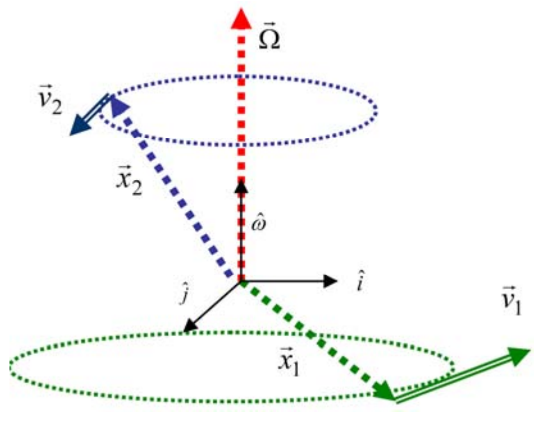

Fig. 1. The antenna array and kinematics in a rotation-only vehicle.

Using Doppler observations derived from the carrier phase, we can estimate the velocity of each antenna, $\vec{v}_1$ and $\vec{v}_2$, using (4). We already know the geometry of the antenna array so the length of each baseline and the dot product magnitude of the two vectors can be used as constraints as shown in (5) and (6).

$$\vec{x}_1 \cdot \vec{x}_2 = c, \tag{5}$$

$$|\vec{x}_1|\ |\vec{x}_2| \ \text{ is known,} \tag{6}$$

where $\vec{x}_1$ and $\vec{x}_2$ are the baseline vectors from the center of rotation to the antennas, to be estimated, and c is the dot product magnitude of them.

We have assumed a rigid antenna platform that rotates about a fixed axis, so each antenna velocity can be obtained by the cross product of an angular velocity of the body $\vec{\Omega}$ and the baseline vector as expressed in (7) and (8).

$$\vec{v}_1 = \vec{\Omega} \times \vec{x}_1, \tag{7}$$

$$\vec{v}_2 = \vec{\Omega} \times \vec{x}_2. \tag{8}$$

Both velocities are perpendicular to $\vec{\Omega}$, so their vector product can indicate $\vec{\varpi}$, the directional unit vector of $\vec{\Omega}$.

$$\vec{\varpi} = \frac{\vec{v}_1 \times \vec{v}_2}{|\vec{v}_1 \times \vec{v}_2|}. \tag{9}$$

Using the estimated unit vector of the rotational axis, we can write the baseline vectors as:

$$\vec{x}_1 = \alpha\ \vec{e}_\alpha + \beta\ \vec{\varpi}, \tag{10}$$

$$\vec{x}_2 = \gamma\ \vec{e}_\gamma + \delta\ \vec{\varpi}, \tag{11}$$

where the following apply.

$\vec{e}_\alpha$ and $\vec{e}_\gamma$: projection of vectors $\vec{x}_1$ and $\vec{x}_2$ onto the plane that is perpendicular to the estimated angular axis

α and γ : component of $\vec{x}_1$ and $\vec{x}_2$ along $\vec{e}_\alpha$ and $\vec{e}_\gamma$,

β and δ : component of $\vec{x}_1$ and $\vec{x}_2$ along $\vec{\varpi}$.

According to the vector algebra, we can estimate $\vec{e}_\alpha$ and $\vec{e}_\gamma$ by the cross product of the estimated velocity and angular axis unit vector as shown in (12).

$$\frac{(\vec{\Omega} \times \vec{x}_1) \times \vec{\varpi}}{|(\vec{\Omega} \times \vec{x}_1) \times \vec{\varpi}|} = \frac{\vec{v}_1 \times \vec{\varpi}}{|\vec{v}_1 \times \vec{\varpi}|} = \vec{e}_\alpha, \quad \frac{\vec{v}_2 \times \vec{\varpi}}{|\vec{v}_2 \times \vec{\varpi}|} = \vec{e}_\gamma. \tag{12}$$

Now that we have derived all the directional vectors, the only remaining issue is the estimation of the scalar components α, β, γ, and δ. The velocity is the cross product of angular velocity and baseline, and $\vec{e}_\alpha$ and $\vec{e}_\gamma$ are perpendicular to $\vec{\Omega}$. The magnitude of each velocity can be rewritten as (13) and (14).

$$\alpha|\Omega| = |\vec{v}_1|, \tag{13}$$

$$\gamma|\Omega| = |\vec{v}_2|. \tag{14}$$

Then we can obtain the ratio between α and γ using the magnitudes of the two antenna velocities regardless of the $|\vec{\Omega}|$ value estimation.

$$\therefore \frac{\alpha}{\gamma} = \frac{|\vec{v}_1|}{|\vec{v}_2|} = c_1. \tag{15}$$

The geometrical constraint (5) can be expressed in terms of α, β, γ, and δ as:

$$\vec{x}_1 \cdot \vec{x}_2 = \alpha\ \gamma\ (\ \vec{e}_\alpha \cdot \vec{e}_\gamma) + \beta\delta = c. \tag{16}$$

Here we know the relationship between $\vec{e}_\alpha$ and $\vec{e}_\gamma$ from (12), and let it be c_2 as shown in (17). Substituting (15) and (17) to (16), we reduce the number of parameters to be estimated as shown in (18).

$$\vec{e}_\alpha \cdot \vec{e}_\gamma = c_2, \tag{17}$$

$$(\beta\delta)^2 = (c - c_1\ c_2\gamma^2\ )^2. \tag{18}$$

Other constraint equations (the baseline lengths), $|\vec{x}_1|$ and $|\vec{x}_2|$, can be rewritten as:

$$\left.\begin{aligned} \beta^2 &= |\vec{x}_1|^2 - (c_1\gamma)^2 \\ \delta^2 &= |\vec{x}_2|^2 - \gamma^2 \end{aligned}\right\}. \tag{19}$$

Using (18) and (19), we finally succeed in making a polynomial equation (20) with one variable from various estimations and constraints.

$$(|\vec{x}_1|^2 - c_1^2\gamma^2)(|\vec{x}_2|^2 - \gamma^2) = (c - c_1\ c_2\gamma^2\ )^2, \tag{20}$$

$$A\gamma^4 + B\gamma^2 + C = 0, \tag{21}$$

where

$$A = c_1^2 - c_1^2 c_2^2,$$

$$B = c_1^2\,|\vec{x}_2|^2 + |\vec{x}_1|^2 - 2cc_1c_2,$$

$$C = |\vec{x}_2|^2\,|\vec{x}_1|^2 - c^2.$$

γ is a solution of the polynomial equation (21) whose degree is 4, and we can estimate the baseline vectors by substituting γ to the (10) to (19). Since there are four roots to this equation, we should choose one solution from the several candidates that are mirror images to the true attitude.

2.3. Attitude determination for the rotation with translation vehicle

We have considered how the attitude of a rotation-only vehicle can be determined by measurement of the Doppler shift. In the real world, however, it is hard to find such a motion, because the rotation of almost all vehicles is generally accompanied by translation. If we use a differential phase velocity, our previous algorithm is still useful in this case.

To understand attitude determination in a rotation motion involving translation, we show in Fig. 2 the antenna array and the kinematics. A master antenna X_1 is

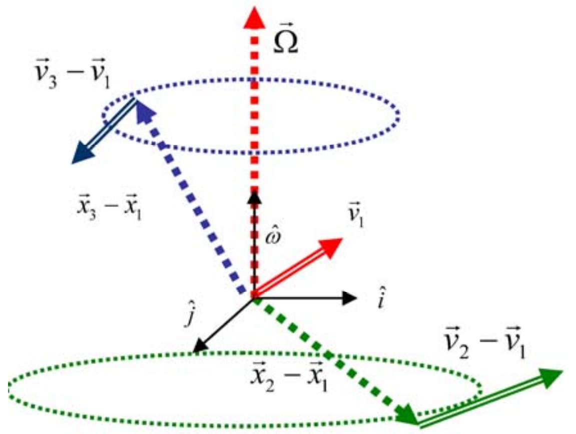

Fig. 2. The antenna array and kinematics in a rotation with transition vehicle.

placed at the center of rotation, and two slave antennas, X_2 and X_3, are located $\vec{x}_2$ and $\vec{x}_3$ from the master. The frame rotates at an angular velocity $\vec{\Omega}$ and translates at linear velocity $\vec{v}_1$.

Recalling that the master antenna is at the rotation center, X_1 has no additional velocity due to the rotation other than $\vec{v}_1$. $\vec{v}_1$ is common to all the antennas, so the differential phase velocities, which are $(\vec{v}_2-\vec{v}_1)$ and $(\vec{v}_3-\vec{v}_1)$, are caused by the rotation. Moreover, this differential phase velocity can reduce the common errors that were explained in (4). The angular velocity of the rigid antenna array appears in the velocity difference equation as:

$$\left.\begin{aligned}\vec{v}_2-\vec{v}_1&=\vec{\Omega}\times(\vec{x}_2-\vec{x}_1)\\ \vec{v}_3-\vec{v}_1&=\vec{\Omega}\times(\vec{x}_3-\vec{x}_1)\end{aligned}\right\}. \tag{22}$$

Equation (22) is very similar to (7) and (8), and $\vec{x}_2-\vec{x}_1$ and $\vec{x}_3-\vec{x}_1$ are the baseline vectors of each slave antenna to be estimated. Therefore, we can determine the attitude of the rotation and translation vehicle in the same manner as that of rotation only.

3. ALGORITHM FOR THE ATTITUDE DETERMINATION IN A SINGLE EPOCH

To pick out the true solution from amongst several geometrical symmetry points, we use the carrier phase measurements. If there is no error in all the antenna velocities, the estimated mirror images should include the true point of each antenna. We can figure out the double- differenced integer ambiguity based on the solution for each candidate as shown in (23) and (24). Using (25) we can check residual ${}_M\Delta_S{}^i\nabla^j\varepsilon$ for each and then we can conclude the minimum residual norm solution as the ambiguity resolution and the attitude determination.

$${}_M\Delta_S{}^i\nabla^j d={}^i\nabla^j e\cdot\vec{X}_{MS}, \tag{23}$$

where

M,S : master and slave antenna,
i,j : index of satellites,
${}_M\Delta_S{}^i\nabla^j d$: double-difference geometric range,
${}^i\nabla^j e$: single-difference line-of-sight,
$\vec{X}_{MS}$: estimated baseline vector.

$${}_M\Delta_S{}^i\nabla^j N=({}_M\Delta_S{}^i\nabla^j\phi-{}_M\Delta_S{}^i\nabla^j d)/\lambda, \tag{24}$$

where

${}_M\Delta_S{}^i\nabla^j N$: double-difference integer ambiguity,
λ : wavelength of L1 carrier phase.

$$\begin{aligned}{}_M\Delta_S{}^i\nabla^j\varepsilon&={}_M\Delta_S{}^i\nabla^j\phi\\&\quad-({}_M\Delta_S{}^i\nabla^j d+{}_M\Delta_S{}^i\nabla^j N\cdot\lambda).\end{aligned} \tag{25}$$

However, in reality the error in Doppler shift derived from the carrier phase propagates into the velocity and baseline estimation. Generally, the estimation error is increased when the frame rotates slowly, and a long perpendicular distance to the rotational axis creates a large error. The error is occasionally greater than the wavelength of the carrier phase, so we should make a search space for each baseline candidate.

Among the candidates, we first remove inappropriate integers that do not satisfy the geometrical constraint of the antenna array as in (6). After this geometrical constraint test, we do a chi-square threshold test of the residual error to determine whether a candidate integer set is within the probable boundary of the true integer set. The number of the remaining candidates, which pass through these processes, is generally only 1~3. If there remains only one candidate integer set, we regard it as a solution. Otherwise, the remaining candidates should pass a ratio test using F-distribution as a final stochastic verification. We finally resolve the integer ambiguity, and then the relative antenna positions are determined.

Once the relative antenna positions in the local-level navigation frame are known, the attitude angles can be calculated by direct conversion formulas in a direct computation method (DCM) in which the order of rotation is taken into account.

$$\left.\begin{aligned}heading&=\tan^{-1}\left(\frac{x_1}{y_1}\right)\\ pitch&=\tan^{-1}\left(\frac{z_1}{\sqrt{x_1^2+y_1^2}}\right)\\ roll&=-\tan^{-1}\left(\frac{z_2''}{x_2''}\right)\end{aligned}\right\}, \tag{26}$$

where the following apply.

(x_1,y_1,z_1): Local frame components of baseline $\vec{X}_{21}$
(x_2'',y_2'',z_2''): Local frame components of baseline $\vec{X}_{31}$ rotated twice (heading and pitch).

4. SIMULATION

4.1. Simulation descriptions

We did simulations to verify the efficacy of our new algorithm which is summarized in Fig. 3. Through the constraint test using geometrical approach, we can remove unacceptable the antenna geometry sets. Chi-square test can reject stochastically wrong ambiguity candidates, and all the threshold value are based on the previous studies [5]. If the final candidate sets can satisfy the ratio test, the cycle ambiguity is resolved to determint the attitude. If no candidate is remained after all the tests, we regards the ambiguity resolution in the epoch as a failure.

We modeled the GPS attitude receiver SNUGLADR-v2.0 developed on Zarlink GP2000 series chipsets and a S3C2410 microprocessor with an ARM920T core (Jang and Kee 2006). Fig. 4 illustrates the set of 48-channel receiver for the attitude determination and antenna array mount to be modeled for this simulation. Since in this paper we consider the feasibility of our new algorithm, we decided to exclude any redundancy effect. In other words we considered only three single frequency antennas, not four or more dual frequency antenna arrays as generally used in other systems.

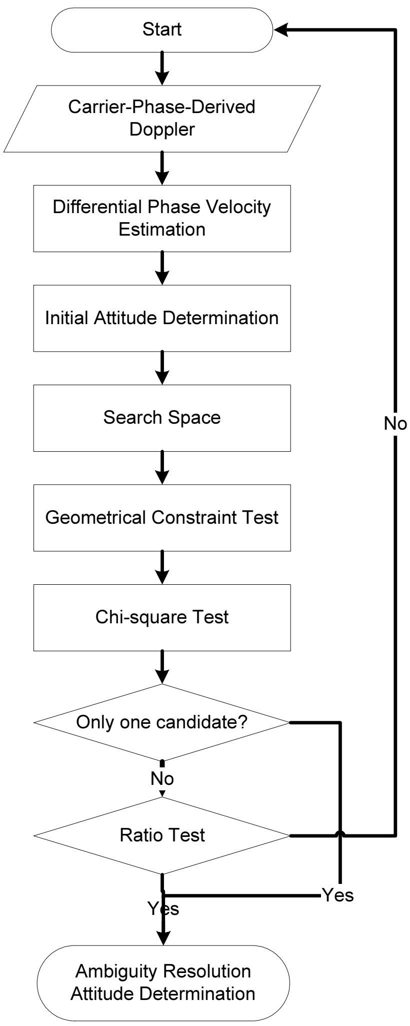

Fig. 3. Block diagram of the attitude determination using doppler.

As summarized in Table 1 the satellite positions and clock bias were calculated at the Young-ju Korean National DGPS reference station in July 2005. The atmospheric errors and receiver clock bias were also considered. The noise pattern of the SNUGLADR-v2.0 was modeled by an exponential function, and its parameters were estimated by the Double Difference method [6] as summarized in Table 2.

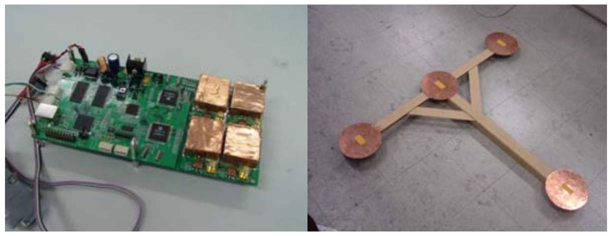

Fig. 4. GPS attitude receiver and antenna array considered in simulation.

Table 1. Summary of simulation construction.

Location (Zero Baseline)	SNU, Seoul (37° 27'03.600"N, 126° 57'06.001"E, 217.965m)
SV Position, & clock bias	Observed at YoungJu Korean NDGPS Reference Station (16th July 09:00, 2005 ~ 17th July 09:00, 2005)
Ionospheric Error	Klobuchar Model (Parameters of 16th July, 2005)
Tropospheric Error	RTCA-recommended Model
Clock Bias	Linearly Increase
Observation Noise	Noise Model of SNUGLADR-v2.0

Table 2. Parameters for the measurement noise model (SNUGLADR-v2.0).

	x_0	x_1	x_2
$\sigma_{\rho 1}$	**0.34**	**1.2**	**12.1**
$\sigma_{\phi 1}$	**0.0028**	**0.0069**	**20.1**

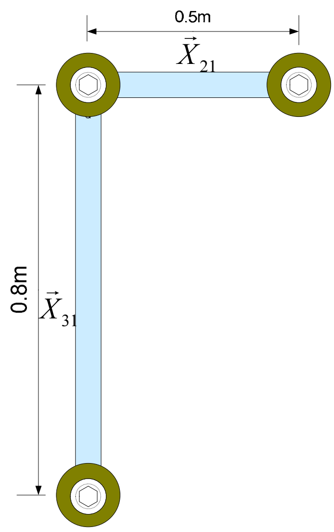

Fig. 5. The antenna array of the simulation.

We modeled the antenna array as in Fig. 4, so we set a master antenna X_1 at the center of rotation 0, 0, 0, one slave antenna X_2 at 0, 0.5, 0, and the other, X_3, at 0.8, 0, 0 as shown in Fig. 5.

The performance of an attitude determination can be determined by its availability, reliability, and accuracy. Once the cycle ambiguity is resolved, the accuracy depends on the noise level of the receiver and the filtering technique, and the reliability should be dealt with by a validation process. The availability of an attitude solution depends on the validation time of integer ambiguity candidates and this is our focus in this paper. In this sense, the time-to-first-fixed-attitude (TTFFA), which is defined as the period from the restart of the attitude algorithm, is a good parameter to be considered.

In reality, we considered various motion scenarios. We first considered constant yaw motion with various magnitudes of angular velocity. Secondly, we examined the success rate of achieving a valid attitude for various rotation axes.

4.2. Simulation 1 – variation in the magnitude of the angular velocity

We can reasonably expect that the magnitude of angular velocity influences our system performance. The velocity error for each antenna has a relatively constant noise level, but its effect with a slowly rotating vehicle is large. The estimation error is therefore increased when the frame rotates slowly. The error included in the estimated angular velocity propagates into the baseline vector estimation, so a long perpendicular distance to the rotational axis creates a large error. In this simulation, we made a rotating frame with a constant yaw motion with varying angular velocity as shown in Fig. 6.

Table 3 summarizes the results of this simulation, and 'Number of final candidates' means that of the remaining candidate integer sets after the geometric constraint and residual chi-square test. As we expected, the velocities of cases 1 and 2 are sufficiently high to reduce the number to only one. There is no other choice than the last remaining integer set, so we do not need to use the ratio test and succeed in resolving the ambiguity in one epoch for the whole simulation. In case 3, we can confirm that the arm length relative to the rotation axis is a factor in the performance. Even with the vehicle rotating very slowly at one revolution per 100 s, the success rate in achieving a valid ambiguity resolution in one epoch is about 97%.

4.3. Simulation 2 – variation in the angular axis

We also examined the success rate of obtaining a valid attitude in various rotation axes as illustrated in Fig. 7. The angular velocity for all cases was the same, $\frac{2\pi}{20}$ rad/s, but the directional vector of the rotation axis differed.

Case 1: rotation axis = (0, 0, 0.3142)
Case 2: rotation axis = (0.1571, –0.2356, 0.1351)
Case 3: rotation axis = (–0.2733, 0.0785, 0.1351)

As we have shown before, a long perpendicular distance to the rotational axis creates a large error. Considering the geometry of the antenna array and each rotation axis, then we can easily understand the result in Table 4. The perpendicular distance of $\vec{X}_{31}$ to the axis in case 2 was 0.6928 m whereas that of $\vec{X}_{21}$ was 0.3307

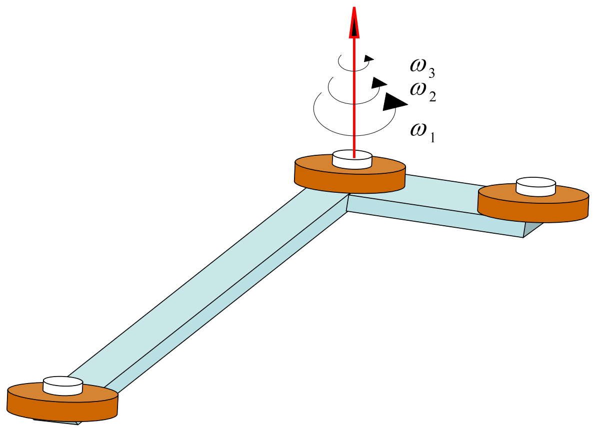

Fig. 6. Scenario of simulation 1.

Table 3. Success rate of valid attitude determination in one-epoch for various angular velocity.

$\lvert\vec{\Omega}\rvert$ (rad/s)		Success rate (%)		Number of final candidates
		$\vec{X}_{21}$ (0.5m)	$\vec{X}_{31}$ (0.8m)	
1	2π/10	100%	100%	1
2	2π/30	100%	100%	1
3	2π/50	100%	99.2%	1-2
4	2π/100	99.6%	97.1%	1-2

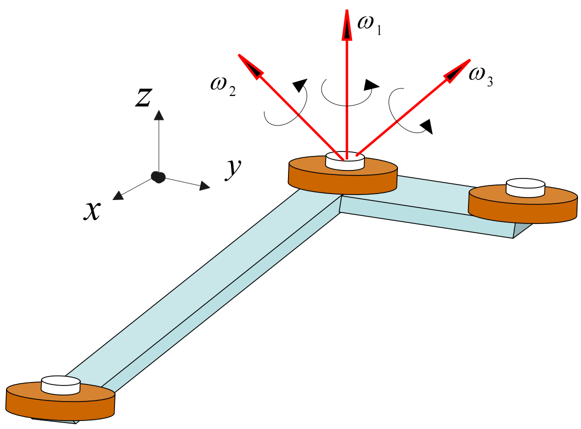

Fig. 7. Scenario of simulation 2.

Table 4. Success rate of valid attitude determination in one-epoch for various rotation axis.

$\vec{\Omega}$		Success rate (%)	
		$\vec{X}_{21}$ (0.5m)	$\vec{X}_{31}$ (0.8m)
1	2π/20 x (0,0,1)	100%	100%
2	2π/20 x (0.5,-0.75,0.43)	99.8%	98.8%
3	2π/20 x (-0.87,0.25,0.43)	99.4%	99.4%

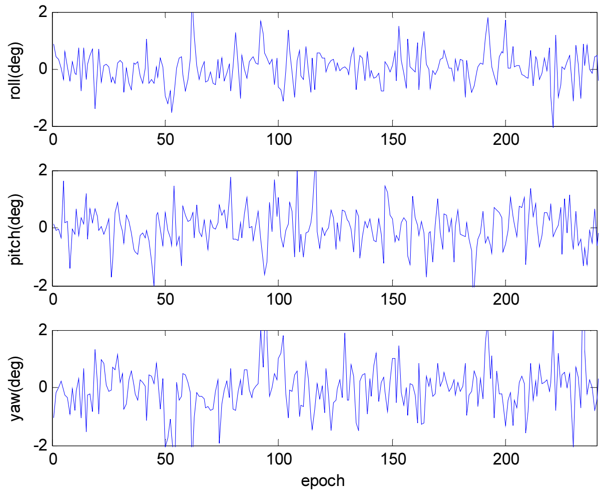

Fig. 8. Attitude error in case 2 of simulation 2.

Table 5. Statistics of attitude error in case 2 of simulation 2.

	Roll(deg)	Pitch(deg)	Yaw(deg)
RMS	0.6090	0.8353	0.7120

m such that the $\vec{X}_{31}$ baseline positioning failed more frequently than with $\vec{X}_{21}$. In case 3, the perpendiculars of $\vec{X}_{21}$ and $\vec{X}_{31}$ were 0.4841 m and 0.3944 m, respectively. These measurements are relatively similar, so the success rates for them were similar. Even if the rotational axis tilts from the yaw axis, the success rate of valid ambiguity resolution for one epoch is seen to be about 99%. The results of attitude error determination in case 2 are shown in Fig. 8 and Table 4.

4.5. Comparison with the performance of the off-the-shelf receiver

To compare the performance of our algorithm, we introduced the results of the PolarRx2 receiver in Table 6. It is very similar to our simulation model because the receiver has one main antenna with two slaves, and because it also uses a DCM. The attitude accuracy depends on the noise level of the receiver after resolving the valid ambiguity. Therefore, the validation time of integer ambiguity candidates is an important performance indicator of the attitude determination algorithm.

According to the simulation results, our algorithm does not fail to resolve the ambiguity in two consecutive epochs. In other words, the maximum TTFFA of our algorithm is only two seconds. The capabilities of making one-epoch fix with the two systems are similar, but our system can resolve the ambiguity more robustly in a shorter time, while general receivers occasionally take more than 30 second as described in Table 6.

Table 6. Test results for TTFFA of PolarRx2 [7].

TTFFA				Wrong fixes
1 epoch	< 30 s	< 150 s	> 150 s	
97.5%	1.0%	0.5%	1.0%	0.3%

5. CONCLUSIONS

The fixing process for cycle ambiguity is an important issue in attitude determination using multiple GNSS antennas. Many researchers try to reduce the computation load in the validation of the ambiguity resolution. In this sense the Doppler shift, especially the Doppler effect derived from the carrier phase, would be a helpful measure, because it contains neither ambiguity nor great noise.

We have proposed a new algorithm to determine the attitude of a rotating vehicle using Doppler measurement. We first estimate the differential phase velocity, and then determine pairs of the unit vector in the rotational axis. Using the estimated axis and geometrical constraints, we can estimate the baseline vectors for each axis vector. In the absence of the measurement noise we can choose the correct solution from among the mirror images. In the real system, however, there exist errors in measurement and estimation, so we made several integer candidate sets that is far fewer than the existing algorithm to find the true solution after engaging chi-square and ratio tests.

To verify our algorithm we carried out two simulations. For all the cases in these simulations, the probability of one-epoch fixes is greater than 97%. Moreover, we did not fail to resolve the ambiguity in two consecutive epochs. In other words, the maximum TTFFA of our algorithm is only two seconds.

Our algorithm is therefore helpful in initial ambiguity resolution in a rotational vehicle. It can reduce the computation load for a complex maneuver. Our method gets better performance when it is applied at faster vehicle, while carrier phase based attitude determination method generally gives better results for slow angular velocity. Therefore, it can be a good complementary to the existing algorithms. In the case of phase lock loss due to rapid spin it can determine the attitude quickly and reliably. Considering that general GPS attitude determination systems are implemented with four antennas or more, the performance of our system is enhanced through hardware redundancy represented by extra antennas or dual frequency signals, and our algorithm can be considered a smart backup technique for attitude determination in an emergency maneuver.

REFERENCES

[1] J. Jang, *Development of a Real-time GNSS Attitude Determination Algorithm and Verification through Hardware Development*, Ph.D. Thesis, Seoul National University, 2006.

[2] P, Misra and P. Enge, *Global Positioning System-Signals, Measurements, and Performance*, 2nd editoin, Ganga-Jamura Press, Massachusetts, pp. 147-275, 2001.

[3] B. Remondi, "Computing satellite velocity using the broadcast ephemeris," *GPS Solutions*, vol. 8, pp. 181-183, 2004.

[4] L. Serrano, D. Kim, R. B. Langley, K. Itani, and M. Ueno, "A GPS velocity sensor: how accurate can it be? – a first look," *Proc. the Institute of Navigation*

National Technical Meeting, San Diego, CA, pp. 875-885, 2004.
[5] J. Jang and C. Kee, "Verification of a real-time attitude determination algorithm through development of 48 channel GPS attitude receiver hardware," *Proc. of the Institute of Navigation NTM*, Monterey CA, pp. 236-243, 2006.
[6] B, Park and C. Kee, "Simplified noise modeling of GPS measurements for a fast and reliable cycle ambiguity resolution," *Proc. of IAIN/GNSS*, Jeju Korea, 2006.
[7] L.V. Kuylen, F, Boon, and A. Simsky, "Attitude determination methods used in the PolaRx2 @ Multi-antenna GPS receiver," *Proc. of the Institute of Navigation GNSS*, Long Beach CA, pp. 125-135, 2005.
[8] C. Park and P. J. G. Teunissen, "Integer least squares with quadratic equality constraints and its application to GNSS attitude determination systems," *International Journal of Control, Automation, and Systems*, vol. 7, no. 4, pp. 566-576, 2009.

Byungwoon Park is a senior researcher at Cadastral Research Institute in Korea Cadastral Survey Corp. He received his B.S., M.S., and Ph.D. degrees from Seoul National University. His research interests include WAD correction algorithms, alternative satellite navigation system, geodesy and RTK-GPS related algorithm.

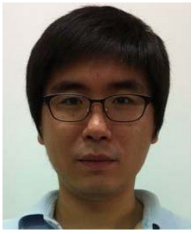

Sanghoon Jeon received his B.S. degree from School of Mechanical and Aerospace Engineering, Seoul National University, Seoul, Korea, in 2004. Currently, He is in Ph.D. course at the School of Mechanical and Aerospace Engineering at Seoul National University. He is the leader of indoor navigation team of GNSS Lab. at Seoul National University. He is interested in GNSS signal processing, attitude determination receiver using GPS, software GNSS receiver.

Changdon Kee is a Professor in School of Mechanical and Aerospace Engineering, Seoul National University, Korea. He received his B.S. and M.S. degrees from Seoul National University and his Ph.D. degree from Stanford University in 1994. He has been involved in GPS research for more than 20 years, during which time he has made numerous contributions, most notably to the development of the Wide Area Augmentation System (WAAS).